

## O–H...O Interactions Involving Doubly Charged Anions: Charge Compression in Carbonate – Bicarbonate Crystals\*\*

Dario Braga,<sup>\*[a]</sup> Emiliana D'Oria,<sup>[a]</sup> Fabrizia Grepioni,<sup>\*[b]</sup> Fernando Mota,<sup>[c]</sup> Juan J. Novoa,<sup>\*[c]</sup> and Concepció Rovira<sup>[c]</sup>

**Abstract:** The O–H...O interaction formed by the anions  $\text{HCO}_3^-$  and  $\text{CO}_3^{2-}$  has been investigated on the basis of data retrieved from the Inorganic Crystal Structure Database (ICSD) and by means of ab initio computations. It has been shown that the O...O separations associated with  $\text{HCO}_3^- \cdots \text{CO}_3^{2-}$  interactions are shorter than those found in crystals containing hydrogen carbonate monoanions such as  $\text{HCO}_3^- \cdots \text{HCO}_3^-$ . Ab initio MP2/6-311G++(2d,2p) computations on the crystal  $\text{Na}_3(\text{HCO}_3)(\text{CO}_3) \cdot 2\text{H}_2\text{O}$  have shown that the interaction between the

monoanion donor and the dianion acceptor, for example  $\text{HCO}_3^- \cdots \text{CO}_3^{2-}$ , is more repulsive than that between singly charged ions, for example  $\text{HCO}_3^- \cdots \text{HCO}_3^-$ , but is largely overcompensated for by anion–cation electrostatic attractions. The shortening of the  $^- \text{O}-\text{H} \cdots \text{O}^{2-}$  interaction relative to the  $^- \text{O}-\text{H} \cdots \text{O}^-$  interaction has been explained as a consequence of the in-

creased *charge compression*, that is of the stronger cation–anion interactions established by the  $\text{CO}_3^{2-}$  dianions with respect to those established by monoanions, and does not reflect an increase in the strength of the  $^- \text{O}-\text{H} \cdots \text{O}^{n-}$  interaction. To expand the structural sample in the crystal packing analysis, the structure of the novel mixed salt  $\text{K}_2\text{Na}(\text{HCO}_3)(\text{CO}_3) \cdot 2\text{H}_2\text{O}$  has been determined by single-crystal X-ray diffraction and compared with the structure of the salt  $\text{Na}_3(\text{HCO}_3)(\text{CO}_3) \cdot 2\text{H}_2\text{O}$  used in the computations.

**Keywords:** ab initio calculations • database analysis • hydrogen bonds • noncovalent interactions

### Introduction

The recent past has witnessed a true explosion of interest in the knowledge, evaluation, and exploitation of intermolecular bonding.<sup>[1]</sup> Today, the investigation of the bonds between molecules and ions involves all areas of chemistry, from supramolecular chemistry<sup>[2]</sup> to biochemistry, to encompass the thriving area of materials chemistry.<sup>[3]</sup>

Strength and directionality are the prerequisites for an intermolecular interaction to be *useful* in a supramolecular or crystal-engineering context.<sup>[4]</sup> The interaction that is commonly accepted to better combine strength and directionality is the hydrogen bond.<sup>[5]</sup> For this reason the hydrogen bond is considered as the masterkey interaction not only in crystal engineering<sup>[6]</sup> and supramolecular<sup>[7]</sup> chemistry, but also in biological systems.<sup>[5a]</sup>

The hydrogen bond is defined as an attractive X–H...Y interaction involving an X–H donor and a Y acceptor group. The formation of these bonds in solution gives rise to well-known shifts in IR bands or in the position of NMR lines, as a consequence of charge transfer from Y to X–H associated with formation of the interaction.<sup>[8]</sup> In crystal structure analysis, on the other hand, hydrogen bonds are usually recognised on the basis of a topological donor–acceptor distance criterion, that is those intra- or intermolecular X–H...Y contacts in which the H...Y distances are shorter than a given threshold separation (generally, the sum of the van der Waals distances of the H and Y atoms) are taken as bona-fide hydrogen bonds. However, previous studies on ionic crystals presenting short  $^- \text{O}-\text{H} \cdots \text{O}^-$  separations between monoanions have shown that the short  $^- \text{O}-\text{H} \cdots \text{O}^-$  contacts are energetically unstable with respect to dissociation in the absence of *external forces* (that is, the counterions)<sup>[9]</sup> thus

[a] Prof. D. Braga, E. D'Oria  
Department of Chemistry G. Ciamician  
University of Bologna  
40126 Bologna (Italy)  
Fax: (+39)051-2099-456  
E-mail: dbraga@ciam.unibo.it

[b] Prof. F. Grepioni  
Department of Chemistry  
University of Sassari  
07100 Sassari (Italy)  
Fax: (+39) 079-212069

[c] Prof. J. J. Novoa, Dr. F. Mota, Dr. C. Rovira  
Departament de Química Física  
Facultat de Química, Universitat de Barcelona  
08028, Barcelona (Spain)  
Fax: (+34)93-402-1231

[\*\*] Queries on the theoretical part should be addressed to Professor J. J. Novoa.

failing to conform to the widely accepted original definition of a bond provided by Linus Pauling.<sup>[10]</sup>

The criticism raised about various aspects<sup>[11]</sup> of this interpretation have been thoroughly addressed in a recent study.<sup>[12]</sup> In summary, the existence of short  $^-O-H\cdots O^-$  contacts between ions carrying like charges is a consequence of the presence of strong attractive cation–anion interactions, energetically stronger than the combined anion–anion and cation–cation repulsions. Such an effect has been called *charge compression*<sup>[13]</sup> and is not confined to hydrogen-bonding interactions between ions of like charges. It has been shown recently that when the X anions present radical properties (that is, the electronic state is of the open shell type) the short  $X\cdots X$  contacts present the same properties that one would expect in energetically stable interactions, although the  $X\cdots X$  interactions alone are energetically repulsive.<sup>[14]</sup>

The analysis of the components of the  $^-O-H\cdots O^-$  interaction energy has revealed that their repulsive nature is due to the strong repulsive nature of the electrostatic component. In a Taylor series expansion of the electrostatic component within the distributed multipole approximation, the leading term is that associated to the electrostatic interaction between the effective charges located on all the atoms forming the  $X\cdots Y$  fragments, whose analytical expression is of the form  $\sum_{ij} q_i q_j / r_{ij}$  ( $i \in X, j \in Y$ ). In this expression, the most important terms are those involving the three atoms participating in the  $X-H\cdots Y$  bond, as these are the ones having the shorter  $r_{ij}$  distance,<sup>[15]</sup> but the other terms are far from negligible. Against what is assumed in many cases, the electrostatic interaction between X anions is *anisotropic*, that is directional. This is due in part to the fact that the summation of all the  $q_i q_j / r_{ij}$  terms is not isotropic, and in part to the anisotropy of the remaining energetic components. Thus, we find that the ionic  $X-H\cdots Y$  interactions have the same directional properties found in the neutral hydrogen bonds, a fact that makes these ionic interactions a powerful tool in the crystal engineering of ionic crystals, particularly in the search for reproducible crystal-directed synthetic strategies.

Herein we extend our study to  $^-O-H\cdots O^{2-}$  interactions where the charge on the acceptor group is increased, thus expectedly increasing the Coulombic repulsion between like charges. The prototype of a fragment showing this interaction is, in the oxoacid family, the hydrogen carbonate-carbonate system, that is  $HCO_3^- \cdots CO_3^{2-}$ . The Inorganic Crystal Structure Database (ICSD)<sup>[16]</sup> contains several crystal structures of salts in which the  $HCO_3^- \cdots CO_3^{2-}$  unit is present. The number of examples, however, is not very large and does not justify full confidence in a

statistical analysis. To widen the sample range under investigation we have also determined the structure of the mixed salt  $K_2Na(HCO_3)(CO_3) \cdot 2H_2O$  and compared it to the structure of the salt  $Na_3(HCO_3)(CO_3) \cdot 2H_2O$ , determined by other workers.<sup>[17]</sup> There is clear evidence that the increase of the charge on the dianion acceptor is associated with a *further shortening* of the  $H\cdots O$  interanionic separation in the  $O-H\cdots O$  contact, relative to that found in similar monoanion–monoanion dimers. Here we will discuss these data, and carry out a detailed theoretical evaluation of the interaction energy involved in the monoanion and dianion cases, using the crystal structure of  $Na_3(HCO_3)(CO_3) \cdot 2H_2O$  as a model.

## Results and Discussion

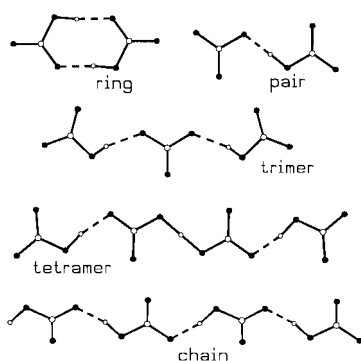
**Topology of the  $HCO_3^- \cdots CO_3^{2-}$  interactions in the solid state:** We have searched the ICSD<sup>[16]</sup> for salts containing the anion  $HCO_3^-$  and the dianion  $CO_3^{2-}$ . The results were manually screened to eliminate all duplicate hits and to subdivide the sample into the two categories of interactions under scrutiny here, namely  $HCO_3^- \cdots HCO_3^-$  and  $HCO_3^- \cdots CO_3^{2-}$ . The geometry of the hydrogen-bonding interactions was evaluated for each structure by means of the program PLATON.<sup>[17]</sup> The data are summarised in Table 1. References to the original structural work can be obtained by consulting the aforementioned database through the code numbers. In the following, only those compounds described in detail or used in the context of this paper will be explicitly quoted. The main packing motifs are shown in Scheme 1.

The salt  $Na_3(HCO_3)(CO_3) \cdot 2H_2O$ <sup>[18]</sup> is one of the few compounds containing *both* the hydrogen carbonate and the carbonate anions. Figure 1 shows that the crystal contains discrete  $HCO_3^- \cdots CO_3^{2-}$  units, which would be more appropriately described as  $[CO_3 \cdots H \cdots CO_3]^{3-}$  units, that is as a sort of super-anion. Indeed the distinction between hydrogen carbonate and carbonate ions is, in this crystal, only semantic: the hydrogen atom of the bridge resides on a centre of inversion and is, therefore, exactly midway between the two oxygen atoms, the  $O\cdots O$  separation being 2.469 Å. The

Table 1. Interionic parameters (distances in Å, angles in °) for the  $HCO_3^- \cdots HCO_3^-$  and  $HCO_3^- \cdots CO_3^{2-}$  interactions in the salts retrieved from the ICSD.

ICSD code	Salt	O–H	(O)H $\cdots$ O	O $\cdots$ O	O–H $\cdots$ O	Motif
100887	NH <sub>4</sub> HCO <sub>3</sub>	0.91	1.69	2.596	168.8	chain
300259	CsHCO <sub>3</sub>	0.86	1.73	2.589	179.9	ring
2325	KHCO <sub>3</sub>	1.00	1.59	2.586	173.0	ring
18183 <sup>[21]</sup>	NaHCO <sub>3</sub>	1.07	1.56	2.610	164.6	chain
				2.595 <sup>[a]</sup>	171.6 <sup>[a]</sup>	
16641 <sup>[18]</sup>	Na <sub>3</sub> (HCO <sub>3</sub> )(CO <sub>3</sub> )·2H <sub>2</sub> O	1.23	1.23	2.469 <sup>[b]</sup>	180.0 <sup>[b]</sup>	pair
2757 <sup>[19]</sup>	KMg(HCO <sub>3</sub> )(CO <sub>3</sub> )·4H <sub>2</sub> O	1.21	1.21	2.425 <sup>[b]</sup>	180.0 <sup>[b]</sup>	pair
401720 <sup>[20]</sup>	Rb <sub>4</sub> (HCO <sub>3</sub> ) <sub>2</sub> (CO <sub>3</sub> )·H <sub>2</sub> O	0.78	1.78	2.525 <sup>[b]</sup>	161.0 <sup>[b]</sup>	trimer
68711 <sup>[22]</sup>	Na <sub>5</sub> (HCO <sub>3</sub> ) <sub>3</sub> (CO <sub>3</sub> )	1.00	1.59	2.572	166.3	tetramer
		1.00	1.60	2.597	180.0	
		1.25	1.25	2.492 <sup>[b]</sup>	171.6 <sup>[b]</sup>	
		1.25	1.25	2.507 <sup>[b]</sup>	180.0 <sup>[b]</sup>	
this paper	K <sub>2</sub> Na(HCO <sub>3</sub> )(CO <sub>3</sub> )·2H <sub>2</sub> O	0.88	1.59	2.468 <sup>[b]</sup>	172.9	pair
				2.515 <sup>[a]</sup>	176.3 <sup>[a]</sup>	

[a] Mean value. [b]  $O_{(HCO_3^-)} \cdots O_{(CO_3^{2-})}$  distance.



Scheme 1. The  $\text{HCO}_3^- \cdots \text{HCO}_3^-$  (ring, chain) and  $\text{HCO}_3^- \cdots \text{CO}_3^{2-}$  (pair, trimer, tetramer) interaction motifs.

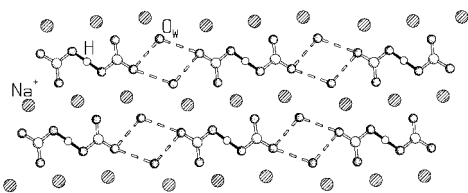


Figure 1. The crystal of  $\text{Na}_3(\text{HCO}_3)(\text{CO}_3) \cdot 2\text{H}_2\text{O}$  is the prototype of the  $\text{HCO}_3^- \cdots \text{CO}_3^{2-}$  interaction. Note how the discrete  $\text{HCO}_3^- \cdots \text{CO}_3^{2-}$  units are more appropriately described as  $[\text{CO}_3 \cdots \text{H} \cdots \text{CO}_3]^{3-}$  super-anions. Shaded atoms represent the cations;  $\text{O}_w$  indicates the water molecules.

packing is completed by two water molecules per formula unit. These water molecules are hydrogen-bridged to the  $[\text{CO}_3 \cdots \text{H} \cdots \text{CO}_3]^{3-}$  units with  $\text{O} \cdots \text{O}$  separations of 2.744 and 2.779 Å. The H atoms belonging to the water molecules were not observed.

Similar  $[\text{CO}_3 \cdots \text{H} \cdots \text{CO}_3]^{3-}$  units are present in the mixed salt  $\text{KMg}(\text{HCO}_3)(\text{CO}_3) \cdot 4\text{H}_2\text{O}$ <sup>[19]</sup> (Figure 2). The trianion bridges the  $\text{Mg}^{2+}$  ions, with  $\text{Mg}^{2+} \cdots \text{O}$  distances equal at

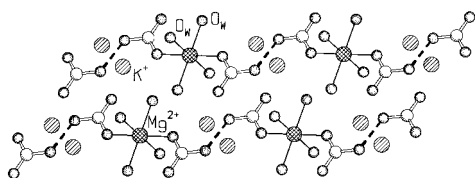


Figure 2. The  $[\text{CO}_3 \cdots \text{H} \cdots \text{CO}_3]^{3-}$  units bridge the  $\text{Mg}^{2+}$  ions in the mixed salt  $\text{KMg}(\text{HCO}_3)(\text{CO}_3) \cdot 4\text{H}_2\text{O}$ . Shaded atoms represent the  $\text{K}^+$  ions;  $\text{O}_w$  indicates the water molecules.

2.057 Å. In coordination network jargon, this arrangement would be described as a noncovalent (hydrogen-bonded) network. The  $\text{Mg}^{2+}$  ions also bear the four water molecules, thus achieving octahedral cocoordination. The  $\text{K}^+$  ions interact with the O atoms of the trianion (shortest  $\text{K}^+ \cdots \text{O}$  distances 2.883 and 2.958 Å). The  $\text{O} \cdots \text{O}$  separation (2.424 Å) within the  $[\text{CO}_3 \cdots \text{H} \cdots \text{CO}_3]^{3-}$  units is the shortest observed in these crystals.

The hydrogen-bridged packing motif in  $\text{Rb}_4(\text{HCO}_3)_2(\text{CO}_3) \cdot \text{H}_2\text{O}$ <sup>[20]</sup> (Figure 3) offers another example of “supramolecular anions”: the carbonate dianion is located in between two hydrogen carbonate units and acts as a bridge through two  $\text{O} \cdots \text{O}$  interactions ( $\text{O} \cdots \text{O}$  distance 2.525 Å).

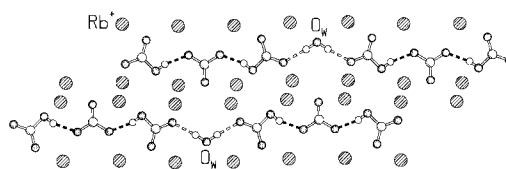


Figure 3. The hydrogen-bridged packing motif in  $\text{Rb}_4(\text{HCO}_3)_2(\text{CO}_3) \cdot \text{H}_2\text{O}$ . The carbonate dianion is in between two hydrogen carbonate units and acts as a bridge through two  $\text{O} \cdots \text{O}$  interactions. Shaded atoms represent the  $\text{Rb}^+$  ions;  $\text{O}_w$  indicates the water molecules.

The  $\text{Rb}^+$  ions interact with the O atoms, with eight  $\text{Rb} \cdots \text{O}$  distances in the range 2.882–2.995 Å.

On further increasing the number of hydrogen carbonate anions with respect to carbonate dianions, the superanion becomes more complex and begins to approach the chain motif observed in  $\text{NaHCO}_3$ <sup>[21]</sup> (see Scheme 1). The structure of  $\text{Na}_5(\text{HCO}_3)_3(\text{CO}_3)$  in fact contains<sup>[22]</sup> a tetraanionic unit that could be regarded as being formed by a central supramolecular trianion of the type depicted in Figure 1 and Figure 2, that is  $[\text{CO}_3 \cdots \text{H} \cdots \text{CO}_3]^{3-}$ , carrying two outer  $\text{HCO}_3^-$  units. This motif is shown in Figure 4, together with the  $\text{Na}^+$  ions.

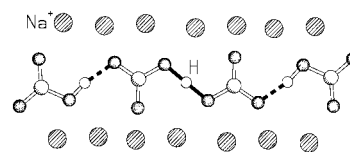


Figure 4. The structure of  $\text{Na}_5(\text{HCO}_3)_3(\text{CO}_3)$  contains oligomers formed by a central supramolecular trianion  $[\text{CO}_3 \cdots \text{H} \cdots \text{CO}_3]^{3-}$  carrying two outer, hydrogen-bridged  $\text{HCO}_3^-$  units. Shaded atoms represent the  $\text{Na}^+$  ions.

The salt  $\text{K}_2\text{Na}(\text{HCO}_3)(\text{CO}_3) \cdot 2\text{H}_2\text{O}$  has been prepared by us (see Experimental Section) and structurally characterised by single-crystal X-ray diffraction. Although the stoichiometry is the same as that of  $\text{Na}_3(\text{HCO}_3)(\text{CO}_3) \cdot 2\text{H}_2\text{O}$ , the presence of two different alkali cations appears to cause significant differences for the  $\text{HCO}_3^- \cdots \text{CO}_3^{2-}$  interactions. Contrary to what is observed for  $\text{Na}_3(\text{HCO}_3)(\text{CO}_3) \cdot 2\text{H}_2\text{O}$ , where the H atom of the dimeric unit lies on a centre of inversion, the  $\text{HCO}_3^- \cdots \text{CO}_3^{2-}$  dimeric unit is not symmetrical (Figure 5), that is cannot be described, as in the previous

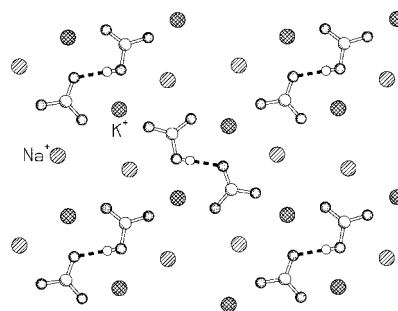


Figure 5. The  $\text{HCO}_3^- \cdots \text{CO}_3^{2-}$  interaction in the structure of  $\text{K}_2\text{Na}(\text{HCO}_3)(\text{CO}_3) \cdot 2\text{H}_2\text{O}$ . Ball and stick representation, note how the H-atom is not located midway along the  $\text{O} \cdots \text{O}$  vector; shaded atoms represent the  $\text{Na}^+$  cations, squared atoms represent the  $\text{K}^+$  ions.

cases, as a supramolecular trianion of the type  $[\text{CO}_3 \cdots \text{H} \cdots \text{CO}_3]^{3-}$  because the hydrogen atom is not located midway along the  $\text{O} \cdots \text{O}$  separation. Even though X-ray diffraction allows location of the electron density of the  $\text{O}-\text{H}$  bond, rather than that of the hydrogen nucleus (for which one should resort to neutron diffraction), the structural data are sufficiently accurate to allow refinement of the hydrogen atom position (see Experimental Section), thus ruling out location of the atom midway along the interaction. This difference is particularly noteworthy, because the  $\text{O} \cdots \text{O}$  separation (2.468(2) Å) is the same as that in  $\text{Na}_3(\text{HCO}_3)(\text{CO}_3) \cdot 2\text{H}_2\text{O}$  (see Table 1). This observation, which is marginal to the subject matter but not irrelevant, *strengthens the idea that there is no direct relationship between location of the H atom along the  $\text{O} \cdots \text{O}$  vector and the strength of the interaction.*<sup>[23, 24]</sup> We agree with Jeffrey, who described the proton in these “strong hydrogen bonding interactions” as “hesitating”.<sup>[5a, 25]</sup> As we have recently pointed out,<sup>[23]</sup> there are no cases of truly symmetrical *intermolecular*  $-\text{OH} \cdots \text{O}^-$  interactions in neutron diffraction structures extracted from the Cambridge Structural Database.<sup>[26]</sup> In all cases where the hydrogen atom is located midway in between the O atoms, the same atom is also located *on a crystallographic symmetry element*, and may thus be a result of the average over space of the diffraction experiment. Further discussion of this aspect is, however, beyond the scope of this article.

There seems to be no apparent relationship between the location of the  $\text{Na}^+$  and  $\text{K}^+$  ions and the position of the hydrogen atom along the  $\text{O} \cdots \text{O}$  vector in crystalline  $\text{K}_2\text{Na}(\text{HCO}_3)(\text{CO}_3) \cdot 2\text{H}_2\text{O}$ . It has been recently reported, however, that the position of the H atom may change along the donor–acceptor vector as a function of the temperature,<sup>[27]</sup> which we have not explored in the present case.

**Theoretical analysis of the crystal packing:** We have previously shown that it is possible to rationalize the structure of any given crystal by looking at the energetics of the dominant interactions between the nearest neighbours by quantum-chemical *ab initio* methods.<sup>[28]</sup> Since the method will not be described in detail here, it is useful to recall that the approach is exact when applied to isolated dimers and is also expected to perform well on aggregates.<sup>[29]</sup> Results on various ionic crystals indicate that the attractive or repulsive nature of the interactions between pairs of fragments is not changed when the first, second or higher coordination shells connected to these fragments are included in the computation.<sup>[29b]</sup> Furthermore, the method makes no assumptions about the sign of the energy associated to each contact, and on its dependence on the nature of the nearby groups. Thus, for instance, an  $\text{O}-\text{H} \cdots \text{O}$  contact in an isolated dimer can change its strength and sign depending on the type of fragments to which it is attached, being moderately attractive when the two fragments are neutral (as in the water dimer), to strongly attractive if the O-acceptor is part of a negatively charged ion, or repulsive when the  $\text{O}-\text{H}$  and O fragments both have negative signs.<sup>[30]</sup> A similar behaviour is expected to hold when the dimer is part of a large aggregate, as we have recently demonstrated.<sup>[12]</sup>

To understand the increase in the  $\text{O}-\text{H} \cdots \text{O}$  charge compression as the charge on the anions is increased, we

compared the energetics of the  $\text{HCO}_3^- \cdots \text{CO}_3^{2-}$  fragment found in the crystal of  $\text{Na}_3(\text{HCO}_3)(\text{CO}_3) \cdot 2\text{H}_2\text{O}$ <sup>[18]</sup> with the energetics of the  $\text{HCO}_3^- \cdots \text{HCO}_3^-$  fragment present in the  $\text{NaHCO}_3$  crystal.<sup>[12]</sup> We evaluated the interaction energy of the  $\text{HCO}_3^- \cdots \text{CO}_3^{2-}$  fragment using the MP2 method and the 6-311G++(2d,2p) basis set (no counterpoise correction was made, as our previous studies have shown that ionic interactions present small basis set superposition errors (see Experimental Section)). The interaction energy of this fragment is found to be repulsive by 75.2 kcal mol<sup>-1</sup>, therefore the stability of the crystal has to come from the cation–anion interactions. There are twelve first neighbour  $\text{Na}^+$  ions surrounding the  $\text{HCO}_3^- \cdots \text{CO}_3^{2-}$  fragment (see Figure 6a).

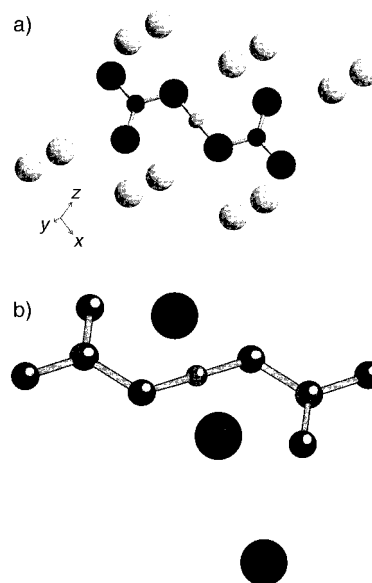


Figure 6. a) The twelve first neighbour  $\text{Na}^+$  ions surrounding the  $\text{HCO}_3^- \cdots \text{CO}_3^{2-}$  fragment in the  $\text{HCO}_3^- \cdots \text{CO}_3^{2-} \cdots [\text{Na}^+]_{12}$  cluster. b) The  $\text{HCO}_3^- \cdots \text{CO}_3^{2-} \cdots [\text{Na}^+]_3$  aggregate used in the computations.

The sodium atoms are placed above and below the plane of the  $\text{HCO}_3^- \cdots \text{CO}_3^{2-}$  fragment, forming four groups of three atoms, distributed in such a way that they form a square when seen along the C–C line of the  $\text{HCO}_3^- \cdots \text{CO}_3^{2-}$  dimers. The shortest  $\text{Na}^+ \cdots \text{O}$  distances to the nearby O atom are in the range 2.376–3.957 Å. This  $\text{HCO}_3^- \cdots \text{CO}_3^{2-} \cdots [\text{Na}^+]_{12}$  aggregate contains more sodium atoms than required to reflect the correct stoichiometry in the crystal, as some of the sodium atoms are shared with nearby  $\text{HCO}_3^- \cdots \text{CO}_3^{2-}$  dimers. Therefore, for our studies we chose the  $\text{HCO}_3^- \cdots \text{CO}_3^{2-} \cdots [\text{Na}^+]_3$  aggregate shown in Figure 6b, which is one of the possible minimal units from which the crystal of  $\text{Na}_3(\text{HCO}_3)(\text{CO}_3) \cdot 2\text{H}_2\text{O}$ <sup>[17]</sup> can be obtained by translation in three-dimensional space. This  $\text{HCO}_3^- \cdots \text{CO}_3^{2-} \cdots [\text{Na}^+]_3$  aggregate can be taken as a good model to evaluate the cation–anion interactions and the energetic stability of the crystal. At the MP2/6-311G++(2d,2p) level the six  $\text{Na}^+$ -anion interaction energies are attractive by 92.6, 107.9, 115.4, 154.6, 207.4 and 212.1 kcal mol<sup>-1</sup>, while the interaction energy between the three  $\text{Na}^+$  ions is repulsive by 216.7 kcal mol<sup>-1</sup>. Overall, the aggregate (Figure 6b) is stable by 546.8 kcal mol<sup>-1</sup>.

The previous values can be compared with the overall stability of the  $\text{HCO}_3^- \cdots \text{HCO}_3^-$  dimer in a  $\text{NaHCO}_3$  crystal packed according to a chain motif, as previously shown.<sup>[12]</sup> In such a crystal, the main energetic features can be analysed by looking at the chain  $\text{Na}_2(\text{HCO}_3)_2$  fragment depicted in Figure 7. Once again, this represents the minimum unit from

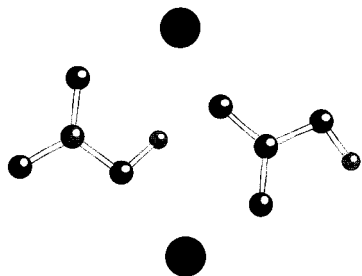


Figure 7. The chain motif in sodium hydrogen carbonate.

which the crystal can be obtained by translation along the three directions of space. At the MP2/6-311G++(2d,2p) level, the  $\text{HCO}_3^- \cdots \text{HCO}_3^-$  dimer is repulsive by  $56.7 \text{ kcal mol}^{-1}$ . The four  $\text{Na}^+$ –anion interactions have attractive interaction energies with the nearest  $\text{HCO}_3^-$  ion of 93.9, 103.2, 118.8 and  $119.7$ , and the  $\text{Na}^+ \cdots \text{Na}^+$  interaction is repulsive by  $67.8 \text{ kcal mol}^{-1}$ . The overall stability of the  $\text{Na}_2(\text{HCO}_3)_2$  fragment is  $287.1 \text{ kcal mol}^{-1}$ , that is about half of the stability of the  $\text{HCO}_3^- \cdots \text{CO}_3^{2-} \cdots [\text{Na}^+]_3$  aggregate.

The previous two sets of numbers show that the isolated anion–anion interactions are repulsive in both aggregates, the  $\text{HCO}_3^- \cdots \text{CO}_3^{2-}$  monoanion–dianion interaction being more repulsive than the  $\text{HCO}_3^- \cdots \text{HCO}_3^-$  case, a fact that fits well with the increase in anionic character and a predominance in the electrostatic component of the interaction energy. However, as shown in Figure 8, the repulsion between these two

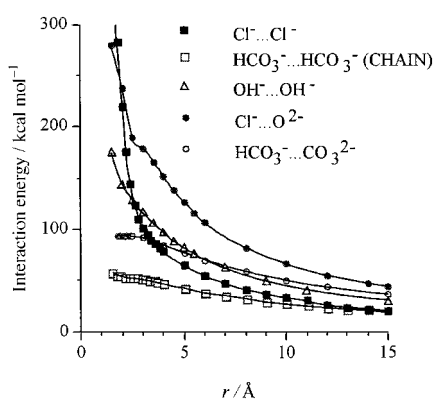


Figure 8. Interaction energy between anions. Note how repulsion between two  $\text{HCO}_3^-$  ions or between  $\text{HCO}_3^-$  and  $\text{CO}_3^{2-}$  is smaller than that between two monoatomic anions of equivalent charge, for example two  $\text{Cl}^-$  ions, or one  $\text{Cl}^-$  and one  $\text{O}^{2-}$  ion.

anions is smaller than that between two monoatomic anions of equivalent charge (two  $\text{Cl}^-$  ions, or one  $\text{Cl}^-$  and one  $\text{O}^{2-}$  ions), that is  $E(\text{HCO}_3^- \cdots \text{HCO}_3^-) < E(\text{Cl}^- \cdots \text{Cl}^-) < E(\text{HCO}_3^- \cdots \text{CO}_3^{2-}) < E(\text{Cl}^- \cdots \text{O}^{2-})$ . For the sake of completeness, we

have also included in Figure 8 the repulsion associated to two  $\text{OH}^-$  ions oriented collinearly in an  $\text{OH}^- \cdots \text{OH}^-$  topology. Given the repulsive nature of the  $\text{HCO}_3^- \cdots \text{CO}_3^{2-}$  interaction, when these two fragments are isolated they necessarily try to dissociate. However, in the presence of cations, the monoanion–dianion repulsion is compensated by the attractive cation–anion interactions and forced towards a stable aggregate, whose geometry is a compromise between all the energetic components of the aggregate. Given that stability, the resulting  $\text{HCO}_3^- \cdots \text{CO}_3^{2-} \cdots [\text{Na}^+]_3$  and  $\text{Na}_2(\text{HCO}_3)_2$  aggregates can be seen as robust packing motifs. These motifs, when translated over space, generate the whole crystal. The  $\text{HCO}_3^- \cdots \text{CO}_3^{2-} \cdots [\text{Na}^+]_3$  aggregate is more stable than the  $\text{Na}_2(\text{HCO}_3)_2$  aggregate because of the larger contribution of the cation–anion interactions, which overcompensate the larger repulsion within the  $\text{HCO}_3^- \cdots \text{CO}_3^{2-}$  fragment with respect to the  $\text{HCO}_3^- \cdots \text{HCO}_3^-$  dimer. The larger overall stability of the cluster allows a shift towards shorter distances in the  $\text{O} \cdots \text{H}$  equilibrium distance in the  $\text{HCO}_3^- \cdots \text{CO}_3^{2-}$  fragment, relative to the value found in the  $\text{HCO}_3^- \cdots \text{HCO}_3^-$  dimer, as found experimentally.

To complete our comparison between the interaction energy in the  $\text{HCO}_3^- \cdots \text{HCO}_3^-$  and  $\text{HCO}_3^- \cdots \text{CO}_3^{2-}$  units, we extended to this latter fragment the energy decomposition analysis performed previously<sup>[12]</sup> to evaluate the energetic components of the total interaction energy. The results of the intermolecular perturbation theory (IMPT) computation (Figure 9) show that the electrostatic component is the

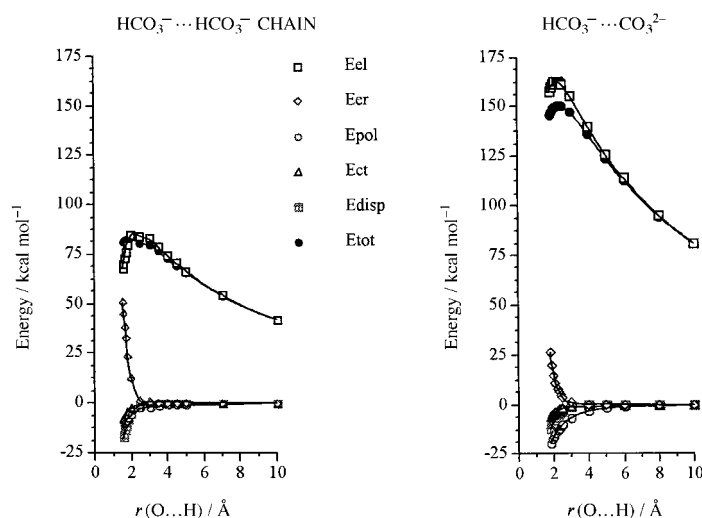
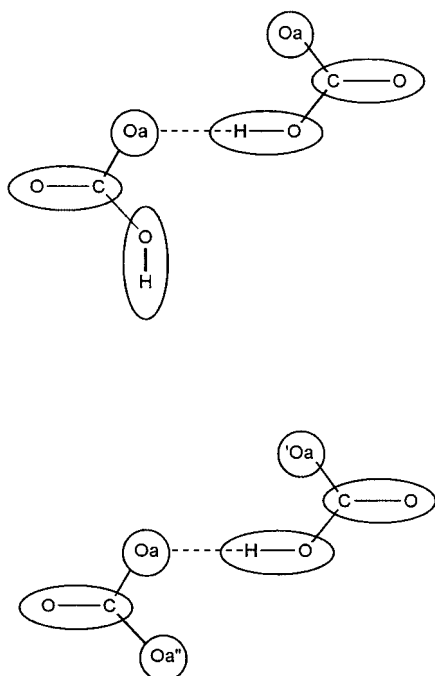


Figure 9. IMPT computation of the components of the interaction energy in the  $\text{HCO}_3^- \cdots \text{HCO}_3^-$  and  $\text{HCO}_3^- \cdots \text{CO}_3^{2-}$  dimers as a function of the  $r(\text{H} \cdots \text{O})$  distance.

dominant one in the  $\text{HCO}_3^- \cdots \text{HCO}_3^-$  and  $\text{HCO}_3^- \cdots \text{CO}_3^{2-}$  units and is even more important in the second fragment, in good agreement with the increase in the net charge. The maximum present at short  $\text{H} \cdots \text{O}$  distance in the  $\text{HCO}_3^- \cdots \text{CO}_3^{2-}$  unit (see Figure 9, right) has the same nature as that in the  $\text{HCO}_3^- \cdots \text{HCO}_3^-$  dimer, which had been previously analysed in detail.<sup>[12]</sup> The remaining terms follow similar patterns in both dimers. We completed our analysis of the

interaction energy by looking in detail at the electrostatic component, which is separated into interaction terms associated with the following fragments: the OH group, the  $O_a$  acceptor atom involved in the  $O-H\cdots O$  contact, the two CO groups, and the remaining O atoms, one of them having an H atom attached to it in the  $HCO_3^- \cdots HCO_3^-$  dimer (see Scheme 2). Each component was computed by using a distributed multipole expansion up to the quadrupole term.



Scheme 2. The  $HCO_3^- \cdots HCO_3^-$  and  $HCO_3^- \cdots CO_3^{2-}$  fragments used in the calculations.

The change in these components as a function of the interfragment  $H\cdots O$  distance is plotted in Figure 10 for both fragments. One can note in Figure 10 that:

- 1) The electrostatic component of the  $O-H\cdots O_a$  interaction is repulsive in both the  $HCO_3^- \cdots HCO_3^-$  and  $HCO_3^- \cdots CO_3^{2-}$  cases. This is in keeping with our previous analysis of the energetic components of the interaction energy in crystals containing  $HCO_3^- \cdots HCO_3^-$  interactions.<sup>[12]</sup>
- 2) The  $O_a \cdots O_a$  interaction is the dominant component in the  $HCO_3^- \cdots HCO_3^-$  fragment and one of the two dominant ones in the  $HCO_3^- \cdots CO_3^{2-}$  fragment, being repulsive in both cases with a similar value.
- 3) The second strongly repulsive component in the  $HCO_3^- \cdots CO_3^{2-}$  fragment comes from the  $O_a \cdots O_a'$  term, which in the  $HCO_3^- \cdots HCO_3^-$  fragment corresponds to the weakly repulsive  $O_a \cdots OH$  component.
- 4) The attractive terms appear to contribute less in the  $HCO_3^- \cdots CO_3^{2-}$  fragment than in the  $HCO_3^- \cdots HCO_3^-$  dimer, although the overall shape is the same in both cases.

As in the  $HCO_3^- \cdots HCO_3^-$  case, the  $HCO_3^- \cdots CO_3^{2-}$  unit shows the existence of molecular orbitals comprising the two fragments indicating electronic delocalisation in spite of the energetically repulsive nature. This means that both types of fragments, although held together by the cation  $\cdots$  anion attractive forces, show electronic properties normally associated with stable hydrogen bonds. On this premise, the hydrogen-bonding interaction between anions within the cluster aggregates  $HCO_3^- \cdots CO_3^{2-} \cdots [Na^+]_3$  and  $Na_2(HCO_3)_2$  can be viewed as *cation-mediated*  $OH\cdots O$  bonds. This view emerges from the fact that, when cations are included in the analysis, these aggregates are energetically stable, hence they can be considered as robust packing motifs.

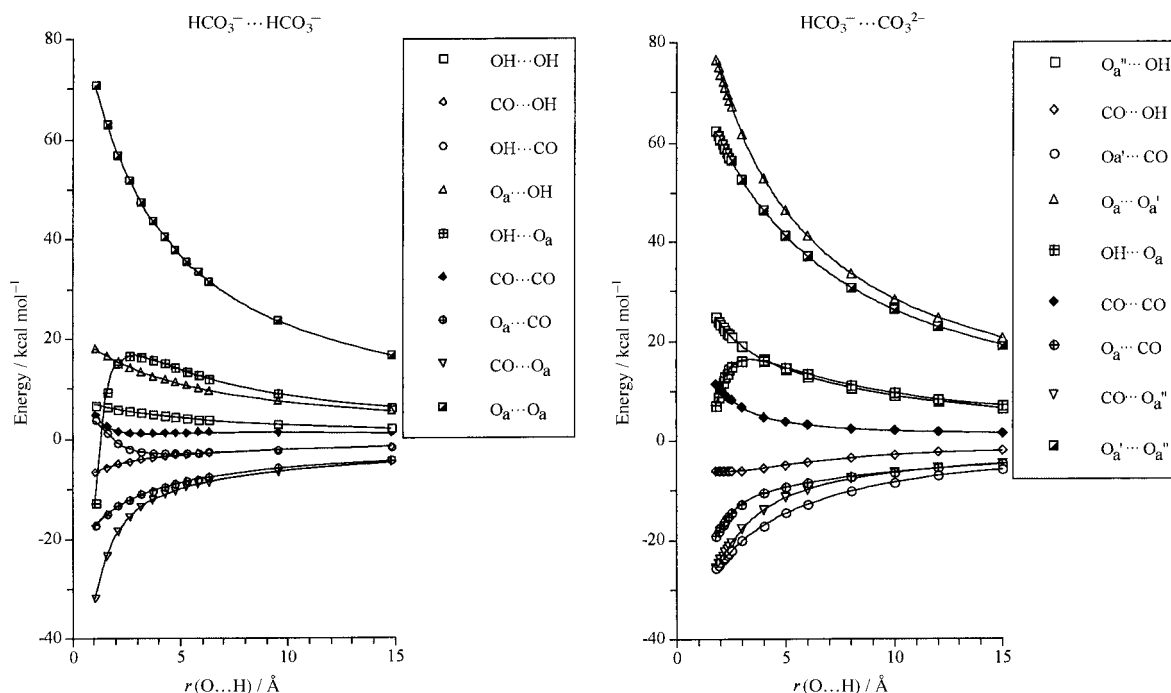


Figure 10. Partitioning of the electrostatic energy component of the interaction energy between the pairs of fragments shown in Scheme 2. The pairs are indicated in the legends.

## Conclusion

The study of the hydrogen bond interaction between anions has much to teach us about the interplay between attractive and repulsive energetic components associated with the simultaneous presence of ions and O–H⋯O hydrogen-bonding interactions. It has been pointed out that it is the overall balance of interactions, some acting at short range only, some acting at very long range, that accounts for cohesion in molecular crystals.<sup>[31]</sup> Our analysis strengthens the idea that non-covalent interactions, their relative strength and their potentials as supramolecular tools, have to be critically evaluated when passing from neutral to charged environments.

Herein we have added further evidence to the fact that the packing choice of small anions capable of hydrogen bond interactions is dictated by two, not necessarily converging, factors: the optimisation of the network of interionic/intermolecular interactions with their directional requirements, and the balance between interionic attractive and repulsive forces. The problem of the nature of  $^-O-H\cdots O^{2-}$  interactions has been tackled by means of topological analysis of known crystal structures and full ab initio computation of the energetics of the interactions involved.

We have shown that the possibility of forming  $^-O-H\cdots O^{2-}$  interactions provides an *additional* stabilisation that adds to the well understood balance of repulsive and attractive energy terms, but does not *determine* crystal cohesion. This contribution is absent in ionic salts where hydrogen bond donors and acceptors are absent, for example NaCl. On the other hand, the  $^-O-H\cdots O^{2-}$  interaction is not per se sufficient to keep ions together and cannot be considered a bona-fide intermolecular bond. Although this may appear a semantic problem, it implies a different appreciation of the energetic hierarchy of the interactions at work in a crystal and in other environments. Perhaps we should take up the suggestion made by Desiraju<sup>[1a]</sup> to go back to the early definition by Huggins of a hydrogen bond as a *hydrogen bridge* (*Wasserstoffbrücke*).<sup>[32]</sup>

## Experimental Section

$K_2Na(HCO_3)(CO_3)\cdot 2H_2O$  was obtained by co-crystallisation in air of an aqueous solution of  $Na(HCO_3)$  and  $K(HCO_3)$  in a 1:1 ratio. Single crystals suitable for X-ray diffraction were obtained by evaporation of the water solution under vacuum. Correspondence between the single-crystal structure described below and the bulk material was ascertained by comparison of the observed powder diffraction pattern with that calculated on the basis of the single crystal structure.

**Crystallography:** Single-crystal X-ray diffraction data of  $K_2Na(HCO_3)(CO_3)\cdot 2H_2O$  were collected at room temperature on a Nonius CAD4 diffractometer equipped with a graphite monochromator ( $Mo_{K\alpha}$  radiation,  $\lambda = 0.71073 \text{ \AA}$ ):  $C_2H_3K_2NaO_8$ ,  $M_r = 258.25$ , orthorhombic,  $Pnma$ ,  $a = 9.336(2)$ ,  $b = 7.894(2)$ ,  $c = 11.417(2) \text{ \AA}$ ,  $V = 841.4(3) \text{ \AA}^3$ ,  $Z = 4$ ,  $F(000) = 520$ ,  $\mu = 1.190 \text{ mm}^{-1}$ ,  $\theta$ -range  $3\text{--}30^\circ$ , 1436 reflections, 1298 independent, refinement on  $F^2$  for 85 parameters,  $R_w(F^2, \text{all refls.}) = 0.1313$ ,  $R_1(I > 2\sigma(I)) = 0.0435$ . The computer program SHELX97<sup>[33a]</sup> was used for structure solutions and refinements based on  $F^2$ . All non H atoms were refined anisotropically and hydrogen atoms were added in calculated positions. SCHA-KAL99<sup>[33b]</sup> was used for all graphical representations. Crystallographic data (excluding structure factors) for the structure

reported in this paper have been deposited with the Cambridge Crystallographic Data Centre as supplementary publication no. CCDC-167977. Copies of the data can be obtained free of charge on application to CCDC, 12 Union Road, Cambridge CB2 1EZ, UK (fax: (+44)1223-336-033; e-mail: deposit@ccdc.cam.ac.uk).

Energetic computations: Ab initio calculations were carried out at the MP2/6-311G++(2d,2p) level, which refers to computations done using the 6-311G++(2d,2p) basis set and the second order Moller–Plesset method (MP2) with Gaussian 98.<sup>[34]</sup> The CPFGA analysis focuses on the packing energy as the sum of the interaction energy between pairs of molecules.<sup>[35]</sup> For ionic interactions, both the Hartree–Fock method and MP2 provide the right order and sign of the interaction energy. The IMPT computations<sup>[36]</sup> were performed using the same basis set in the perturbational Scheme introduced by Hays and Stone.<sup>[36]</sup> IMPT computations give a quantitative and rigorous breakdown of the total energy of each fragment in physically meaningful components: electrostatic, exchange–repulsion, polarization, charge transfer, and dispersion.<sup>[37]</sup> The IMPT method is free of the unwanted basis set superposition errors present in other methods due to the use of truncated basis sets.

## Acknowledgements

D.B. and F.G. thank M.U.R.S.T. (project Solid Supermolecules), the University of Bologna (project Innovative Materials) and the University of Sassari for financial support. J.J.N. thanks DGES (project PB 98-1166-C02-02) and CIRIT (1999SGR 00046) for their support, and CESCACEPBA for the allocation of computer time. Financial support within the “Azione Integrata” between Italy and Spain is acknowledged. We also thank the EU for financial support within the COST-D 11.

- [1] a) G. R. Desiraju, T. Steiner, *The Weak Hydrogen Bond in Structural Chemistry and Biology*, Oxford University Press, Oxford, **1999**; b) D. Braga, F. Grepioni, *Acc. Chem. Res.* **2000**, *33*, 601.
- [2] J. M. Lehn, *Supramolecular Chemistry: Concepts and Perspectives*, VCH, Weinheim, **1995**.
- [3] a) D. Braga, F. Grepioni, A. G. Orpen, *Crystal Engineering: from Molecules and Crystals to Materials*, Kluwer, Dordrecht, **1999**; b) K. T. Holman, A. M. Pirovar, J. A. Swift, M. D. Ward, *Acc. Chem. Res.* **2001**, *34*, 107; c) C. N. R. Rao, S. Natarajan, A. Choudhury, S. Neeraj, A. A. Ayi, *Acc. Chem. Res.* **2001**, *34*, 80.
- [4] a) D. Braga, F. Grepioni, *Chem. Commun.* **1996**, 571; b) A. D. Burrows, C.-W. Chan, M. M. Chowdry, J. E. McGrady, D. M. P. Mingos, *Chem. Soc. Rev.* **1995**, 329; c) S. Subramanian, M. J. Zaworotko, *Coord. Chem. Rev.* **1994**, *137*, 357; d) D. Braga, F. Grepioni, G. R. Desiraju, *Chem. Rev.* **1998**, *98*, 1375; e) M. W. Hosseini, A. De Cian, *Chem. Commun.* **1998**, 727; f) L. Brammer, D. Zhao, F. T. Ladipo, J. Braddock-Wilking, *Acta Crystallogr. Sect. B* **1995**, *51*, 632; g) C. B. Aakeröy, *Acta Cryst. Sect. B* **1997**, *53*, 569; h) M. J. Calhorda, *Chem. Commun.* **2000**, 801.
- [5] a) G. A. Jeffrey, W. Saenger, *Hydrogen Bonding in Biological Structures*, Springer, Berlin, **1991**.
- [6] “The Crystal as a Supramolecular Entity” in *Perspectives in Supramolecular Chemistry, Vol. 2* (Ed.: G. R. Desiraju), Wiley, Chichester, **1996**, p. 107.
- [7] a) J. M. Lehn, *Angew. Chem.* **1990**, *102*, 1347; *Angew. Chem. Int. Ed. Engl.* **1990**, *29*, 1304; b) G. M. Whitesides, E. E. Simanek, J. P. Mathias, C. T. Seto, D. N. Chin, M. Mammen, D. M. Gordon, *Acc. Chem. Res.* **1995**, *28*, 37; c) J. W. Steed, J. L. Atwood, *Supramolecular Chemistry*, Wiley, Chichester, **2000**.
- [8] See, for example: a) H. Umeyama, K. Morokuma, *J. Am. Chem. Soc.* **1977**, *99*, 1316; b) M. S. Gordon, J. H. Jensen, *Acc. Chem. Res.* **1996**, *29*, 536; c) O. N. Ventura, J. B. Rama, L. Turi, J. J. Dannenberg, *J. Phys. Chem.* **1995**, *99*, 131; d) C. Lee, G. Fitzgerald, M. Planas, J. J. Novoa, *J. Phys. Chem.* **1996**, *100*, 7398.
- [9] a) D. Braga, F. Grepioni, J. J. Novoa, *Chem. Commun.* **1998**, 1959; b) D. Braga, F. Grepioni, *New J. Chem.* **1998**, 1159.
- [10] L. Pauling, *The Nature of the Chemical Bond*, Cornell University Press, **1960**, page 6: “There is a chemical bond between two atoms or groups of atoms in the case that the forces acting between them are such

- as to lead to the formation of an aggregate with sufficient stability to make it convenient for the chemist to consider it as an independent molecular species.”
- [11] a) T. Steiner, *Chem. Commun.* **1999**, 2299; b) M. Mascal, C. E. Marajo, A. J. Blake, *Chem. Commun.* **2000**, 1591; c) P. Macchi, B. B. Iversen, A. Sirani, B. C. Chokoumakas, F. K. Larsen, *Angew. Chem.* **2000**, *112*, 2831; *Angew. Chem. Int. Ed.* **2000**, *39*, 2719.
- [12] D. Braga, L. Maini, F. Grepioni, F. Mota, C. Rovira, J. J. Novoa, *Chem. Eur. J.* **2000**, *6*, 4536.
- [13] D. Braga, F. Grepioni, E. Tagliavini, J. J. Novoa, F. Mota, *New J. Chem.* **1998**, 757.
- [14] J. J. Novoa, P. Lafuente, R. Del Sesto, J. S. Miller, *Angew. Chem.* **2001**, *113*, 2608; *Angew. Chem. Int. Ed.* **2001**, *40*, 2540.
- [15] One has to keep in mind the long-distance behaviour of the  $1/r_{ij}$  terms before discarding the remaining interatomic pairs, if an accurate computation of the electrostatic term is desired.
- [16] Inorganic Crystal Structure Database (ICSD), Fachinformationszentrum (FIZ) Karlsruhe and Gmelin Institut, Release 2000/2.
- [17] A. L. Spek, *Acta Crystallogr.* **1990**, *A 46*, C-34.
- [18] R. Candlin, *Acta Crystallogr.* **1956**, *9*, 545.
- [19] G. W. Stephan, C. H. MacGillavry, B. Koch, *Acta Crystallogr.* **1972**, *28*, 1029.
- [20] V. Cirpus, A. Adam, *Z. Anorg. Allgem. Chem.* **1995**, *621*, 1197.
- [21] The structure of sodium hydrogen carbonate is, thus far, the only example of an alkali hydrogen carbonate where a linear chain is observed. For the original structural data see B. D. Sharma *Acta Crystallogr.* **1965**, *18*, 818.
- [22] N. G. Fernandes, R. Tellgren, *Acta Crystallogr.* **1990**, *46*, 466.
- [23] a) D. Braga, J. J. Novoa, F. Grepioni, *New J. Chem.* **2001**, *25*, 226; b) D. Braga, M. Rossini, F. Grepioni, *Cryst. Eng. Comm.* **2001**, *9*.
- [24] a) G. Gilli, F. Bellucci, V. Ferretti, V. Bertolasi, *J. Am. Chem. Soc.* **1989**, *111*, 1023; b) V. Bertolasi, P. Gilli, V. Ferretti, G. Gilli, *Chem. Eur. J.* **1996**, *8*, 925, and references therein.
- [25] G. A. Jeffrey, *An Introduction to Hydrogen Bonding*, Oxford University Press, New York, **1997**.
- [26] F. H. Allen, O. Kennard, *Chemical Design Automation News* **1993**, *8*, 31.
- [27] C. C. Wilson, *Acta Crystallogr. B* **2001**, *57*, 435.
- [28] J. J. Novoa in *Implications of Molecular and Materials Structure for New Technologies* (Eds.: J. A. K. Howard, F. H. Allen, G. P. Shields), Kluwer, Dordrecht, **1999**.
- [29] a) At  $T \neq 0$  K one has also to include entropy increments for a full account of all the driving forces, but we will limit ourselves to the  $T = 0$  case, to simplify the problem; b) J. J. Novoa, F. Mota, unpublished results.
- [30] J. J. Novoa, I. Nobeli, F. Grepioni, D. Braga, *New J. Chem.* **2000**, *24*, 5.
- [31] J. D. Dunitz, A. Gavezzotti, *Acc. Chem. Res.* **1999**, *32*, 677.
- [32] M. L. Huggins, *J. Org. Chem.* **1936**, *1*, 405.
- [33] a) G. M. Sheldrick, SHELXL97, *Program for Crystal Structure Determination*, University of Göttingen, Göttingen, Germany, **1997**; b) E. Keller, SCHAKAL99 *Graphical Representation of Molecular Models*, University of Freiburg, Germany, **1999**.
- [34] a) Revision C.3: M. J. Frisch, G. W. Trucks, H. B. Schlegel, P. M. W. Gill, B. G. Johnson, M. A. Robb, J. R. Cheeseman, T. Keith, G. A. Peterson, J. A. Montgomery, K. Raghavachari, M. A. Al-Laham, V. G. Zakrzewski, J. V. Ortiz, J. B. Foresman, J. Ciolowski, B. B. Stefanov, A. Nanayakkara, M. Challacombe, C. Y. Peng, P. Y. Ayala, W. Chen, M. W. Wong, J. L. Andres, E. S. Replogle, R. Gomperts, R. L. Martin, D. J. Fox, J. S. Binkley, D. J. Defrees, J. Baker, J. J. P. Stewart, M. Head-Gordon, C. Gonzalez, J. A. Pople, Gaussian Inc., Pittsburgh PA, 1995; b) S. Huzinaga, *Gaussian Basis Sets for Molecular Calculations*, Elsevier, Amsterdam, **1984**.
- [35] a) J. J. Novoa, M. Deumal, *Mol. Cryst. Liq. Cryst.* **1997**, *305*, 143; b) M. Deumal, J. Cirujeda, J. Veciana, M. Kinoshita, Y. Hosokoshi, J. J. Novoa, *Chem. Phys. Lett.* **1997**, *265*, 190.
- [36] The acronym IMPT stands for Inter Molecular Perturbation Theory; a) I. C. Hayes and A. J. Stone, *J. Mol. Phys.* **1984**, *53*, 83; b) A. J. Stone, *The Theory of Intermolecular Forces*, Ch. 6, Clarendon Press, Oxford, **1996**.
- [37] Computed using the CADPAC 6.1 code included as part of the UNICHEM 4.1 suite of programs.

Received: July 30, 2001 [F3454]